Reactor network modelling of a close to reality combustor using residence time measurements

M.A. Agizza[1], S. Bürkle [1], L. Becker [1], M. Greifenstein [1], G. Bagheri[4], S. Doost[2], T. Faravelli[4], J. Janicka[2], S. Wagner[3], A. Dreizler [1,*]

[1] Fachgebiet Reaktive Strömungen und Messtechnik, Technische Universität Darmstadt, Germany
[2] Fachgebiet Energie- und Kraftwerkstechnik, Technische Universität Darmstadt, Germany
[3] High Temperature Process Diagnostics, Technische Universität Darmstadt, Germany
[4] Dipartimento di Chimica, Materiali e Ingegneria Chimica, Politecnico di Milano, Italy

Abstract
Residence time distribution measurements in a close to reality configuration devoted to both air and oxyfuel combustion are the starting point to develop a Chemical Reactors Network model. These models support the understanding of the mixing phenomena inside the combustor, and are well suited for performing parametric studies. Differences between the mixing behaviour of air and oxyfuel atmospheres are highlighted.

Introduction

Combustion of fossil fuels dominates the global energy market, and will continue to dominate it in the future, as just a slight decrease is forecasted in the future decades [1]. This has a strong environmental impact that now more than ever has to be minimized. The challenge of combustion research is to explore new ways to reduce pollutant emissions along with high process efficiency. One option lies in a continuous improvement of combustion systems [2], or the application of new combustion concepts, such as oxyfuel combustion. In this concept, air is replaced by a mixture of carbon dioxide (CO_2) and oxygen as oxidizer, leading to an exhaust gas mainly composed of CO_2 and water vapor. The CO_2 can be separated, liquefied and stored underground to reduce the effects on the environment [3].

The development and testing of new processes, as well as the improvement of present technologies needs thorough experimental investigations on properly designed laboratory scale model combustors. Ideally, experimental investigations are complemented by modelling during the design phase of an experiment and for interpretation of results. In this context, computational fluid dynamics (CFD) is nowadays a valuable tool, although computationally costly and unable to deal with detailed kinetic mechanisms. The most important features, namely combustion efficiency and pollutant emissions of combustion-based devices are determined by the complex interaction between turbulence and chemical reactions [4, 5]. Therefore, a somewhat simpler and more flexible tool is needed.

A reactive flow modelling that fits these needs is referred to as Chemical Reactors Networks (CRN). It employs a properly designed arrangement of ideal flow reactors to obtain a simplified version of the flow field inside the combustor. This simplification allows for the use of detailed kinetic mechanisms. A properly designed CRN, from which quantitative species concentrations can be extracted and that enables parametric studies, exploits the Residence Time Distribution (RTD) of the flow. RTD yields the mixing characteristics, which must be reproduced in order to properly describe the reactive flow [6].

In the present study, a CRN is designed, based on RTD measurements of a cold flow in both air and oxyfuel atmospheres. The methodology is applied to better understand the different mixing behaviour due to the different environments inside a laboratory scale model combustor. As future work, the modelling has to be extended to the reactive case, to detect the differences, and to perform parametric studies.

First, the theoretical background and the methodology are introduced, and then the experimental apparatus and the measurement technique are presented. Results from this modelling are discussed following sections.

Background and methodology

The schematization of a combustion chamber by means of a network of properly interconnected ideal flow reactors has been successfully achieved in the past [5-12]. It is still considered a valid tool to complement experimental observations and perform parametric studies with regards to emissions and stability [4, 12-16]. In such a model, the flow field and mixing properties are replaced by an appropriate network of ideal flow reactors, namely the Plug Flow Reactor (PFR) and the Continuous Stirred Tank Reactor (CSTR) [17]. These two ideal chemical reactor models account for two extremes of flow behaviour. The CSTR provides a zero dimensional description of the flow by assuming perfect and instantaneous mixing of all the streams entering the reactor. The PFR represents the opposite behaviour: it employs a one-dimensional approach, in the hypothesis of a piston flow in the stream wise direction and perfect mixing in the generic cross section. In practical situations, such as real industrial reactors or combustors, the actual flow field is more complex, and can be regarded as a network of these ideal reactors, connected in series and parallel. This approach enables the understanding of the main mixing features and the

*Corresponding author: dreizler@rsm.tu-darmstadt.de

employment of detailed kinetic mechanisms to characterize the species formation in the different areas of the combustor, yielding emissions prediction.

Two different methods are available to guide the design of a reactor network. The first method starts from the observation of the flow field and the identification of different zones based on the knowledge of the flow behaviour in the different regions of the combustion chamber [8, 16]. CFD might support the design, by determining the volumes of the reactors and the mass flow among them [4, 6, 12]. These studies have been crucial for the development of a simple, yet powerful, technique for flame modelling. In these previous works, reactor network models suitable for the near nozzle region of both premixed and diffusion flames are proposed [7, 8,18], as well as options for the interaction between combustion zones and cooling air [7].

The other approach to achieve a CRN starts from RTD data [9, 10, 13, 14]. Different fluid elements may take different routes inside the reactor (presence of stagnant regions, bypasses, eddies, etc.), meaning that fluid elements that entered the reactor at the same time will not exit at the same time. This distribution of residence times depends on the mixing characteristics of the system under investigation. The time specific species spend in the respective reactor network governs the completeness of the reaction, as well as the formation of certain pollutants. For this reason, the interpretation of RTD in terms of reactor configuration is a valuable tool to improve the understanding of combustion in practical systems and the development of combustion models for emission and efficiency prediction [10].

RTD can be determined by injecting an inert tracer by means of a pulsed input and recording the concentration at the exit in time, $C(t)$. This kind of experiment enables the direct determination of the RTD, defined as follows [17]:

$$E(t) = \frac{C(t)}{\int_0^{+\infty} C(t)dt} \qquad (1)$$

When a pulse input is experimentally prohibitive, a step input, or a negative step input (also known as washout function) might be used. For a step input, the following equation expresses the temporal evolution of the tracer concentration $C(t)$ at the system outlet:

$$F(t) = C(t)/C_\infty \qquad (2)$$

$F(t)$ is a cumulative density function (CDF), representing the probability for a fluid element injected at t = 0 to exit between t = 0 and time t. C_∞ is the steady state concentration. The relationship between $E(t)$ and $F(t)$ is given by (3):

$$E(t) = \frac{dF(t)}{dt} \qquad (3)$$

As pointed out before, this quantity is a feature of the mixing inside the investigated system. Interpretation of RTD data by means of a network of interconnected ideal flow reactors is therefore an important component in the characterization of a process, employed also to identify reactors shortcomings. This goal can be achieved by first considering the mathematical expression for the $E(t)$ of the simple reactors [19] introduced earlier in this section.

For a CSTR, $E(t)$ is given by equation (4) and illustrated in Figure 1a:

$$E(t)_{CSTR} = \frac{e^{-t/\tau}}{\tau} \qquad (4)$$

A PFR accounts for a delay time, and its RTD is expressed by the Dirac delta function, equation (5) and is shown Figure 1b:

$$E(t)_{PFR} = \delta(t-\tau) \qquad (5)$$

Calculations of exit age distributions for selected non-ideal flows can be found in literature [17, 19], and they are the starting point to design a reactor network for the system under investigation.

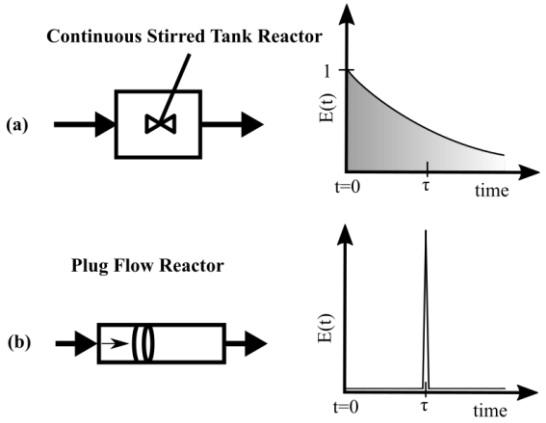

Figure 1 – representation of the ideal flow reactors employed and exemplification of their residence time distribution, $E(t)$.

Zonal modelling by means of flow visualization data, based on either experiments or numerical simulations, supports interpretation of the measured residence time distribution in terms of main flow structures. In addition, interlinking the two methodologies allows to extract physical significance of each reactor i.e., each reactor represents a certain characteristic volume in the system.

Once a CRN whose RTD matches the experimentally measured one is accomplished, the CRN is assumed to represent the mixing features of an enclosed reactor [6]. Therefore, when applied to combustors, this methodology is a tool to analyse species formation trends in different areas of the system, so to yield emission predictions, fuel burnout, or to estimate flame blowout conditions [5]. Furthermore, the exploration of the interaction

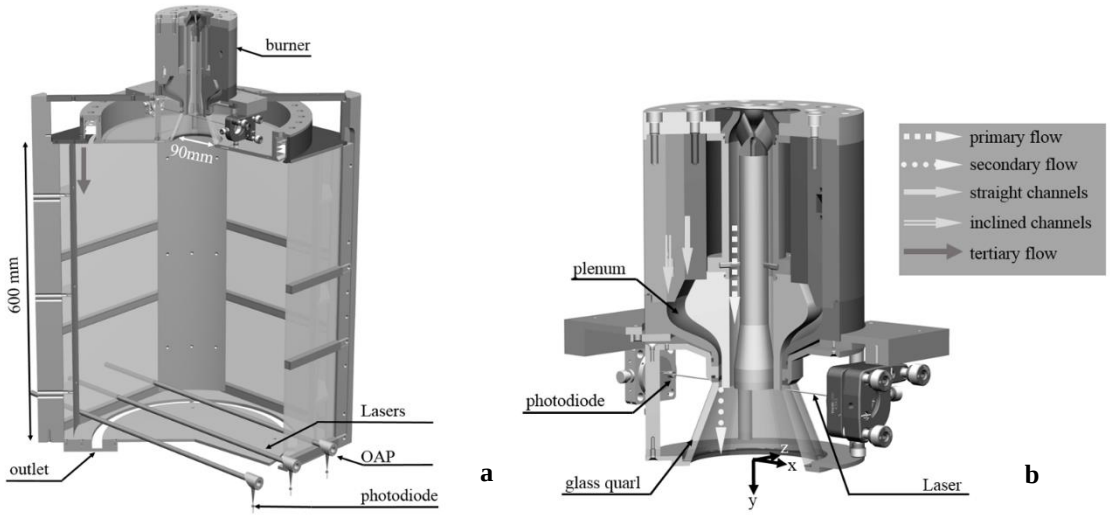

*Figure 2 – **a** – Sectional view of the 20 kW oxyfuel combustion chamber and outlet laser position; **b** – Sectional view of burner, quarl and inlet laser position*

between turbulence and chemical kinetic pathways is possible. Thus, the information provided is useful for the optimization of combustors, to meet both efficiency and emissions regulation criteria.

In the following, RTD data interpretation in conjunction with zonal modelling of the flow is employed, following the work carried out in [13], to achieve a CRN in an intermediate scale close to reality configuration designed at Technische Universität Darmstadt [20, 21].

Experimental apparatus

The test rig under investigation is an intermediate-scale combustor, suitable for operating gas flames as well as gas-assisted coal flames. It is designed to close the gap between unconfined laboratory-scale coal burners and confined industrial-scale coal combustors, and allows the exploration of both air and oxyfuel atmospheres [20]. Figure 2 shows the geometry, and details of about the experimental setup for the RTD measurements. Dimensions are provided in Table 1. The burner down-fires into the combustion chamber. Walls are made of wedged fused silica to enable optical access. Inside the burner quarl, two inlet orifices surround a bluff body (magnification in Fig, 2b): a partially premixed mixture of fuel and oxidizer (air or oxyfuel) is exiting the inner orifice (primary flow, FI), whereas swirled oxidizer issues through the outer orifice (secondary flow, FII). A tertiary flow, FIII, of oxidizer is injected close to the windows (Figure 2a).

Experimental residence time distribution measurements

RTD measurements have been carried out both in non-reactive and reactive conditions, whose operating points are listed in Table 2. CH_4 was injected as gaseous tracer injected in the primary flow orifice (see Figure 2) and was detected in-situ by means of direct tunable laser absorption spectroscopy (TDLAS) [22].

Table 1 – Dimensions of the burner and combustor

Quarl dimensions	[mm]
Larger diameter, D	90
Smaller diameter, d	49.2
Height	53
Combustion chamber dimensions	[mm]
Length	600
Width	420
Depth	420

Table 2 – Operation conditions

Operation points	**NRAIR**	**NR30**
Oxidizer Air/O_2/CO_2 (vol%)	100/0/0	0/30/70
I CH4 (m^3/h)	0	0
I Oxidizer (m^3/h)	13.55	8.16
II Straight Oxidizer (m^3/h)	5.97	3.76
II Inclined Oxidizer (m^3/h)	12.02	7.27
III Oxidizer (m^3/h)	69.95	42.60

The gas phase RTD was measured probing the concentration of CH_4 injected in the primary flow at the inlet and representative positions at the combustor exit simultaneously, using a diode laser. It was shown, that the choice of the tracer had a negligible impact on the flow and the measured tracer response.

Results and discussion

In this section the CRN is presented using measured temporal CH_4 profiles. The network is designed stepwise, as follows:

- interpretation of RTD data, to gain a first understanding of the mixing inside the combustor;
- identification of the main flow features and separation of the flow into zones with well-defined, ideal mixing characteristics [10, 12];
- modelling of the zones by means of ideal flow reactors;

- a PFR is chosen if a prevailing flow direction is present;
- otherwise, a CSTR is associated to the zone [6].

The design of a network based on RTD data interpretation in terms of main flow structures is based on the following constrains:

- the sum of reactor volumes is equal to the furnace volume;
- the flows among the reactors are determined by fitting the calculated RTD curve to the experimental one, using a least square fit. To this aim, each designed system is implemented in Matlab Simulink®.

The determination of the zones volumes and the reactor arrangement is, in this context, semi-empirical, and aided by preliminary RTD analysis. Experimental and numerical flow visualization data (Figure 4 and [20, 21]) aid the schematization of the combustor in terms of main flow structures, building on the tracer response curves, shown in Figure 3.

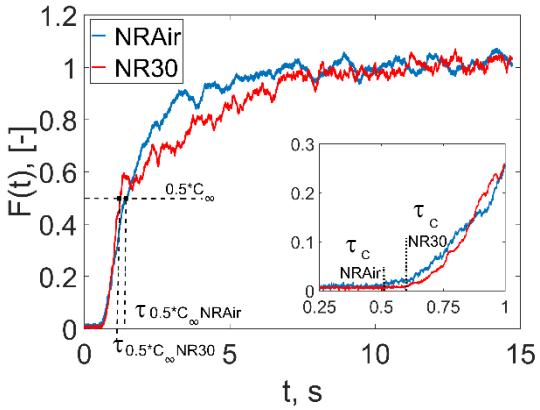

Figure 3 – tracer response from [22], averaged over a series of measurements. Characteristic times listed in Table 3 are also highlighted. The insert shows a magnification of the outlet concentration until t =1 s.

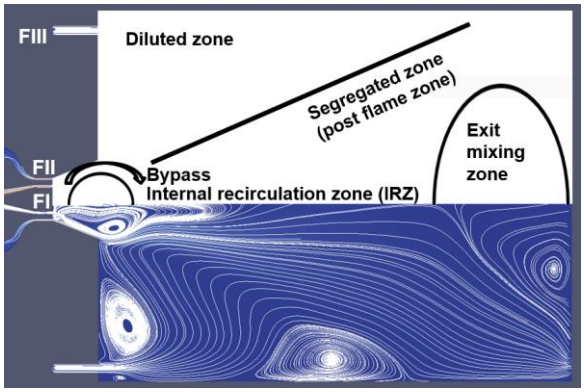

Figure 4 – streamlines for the NRAir case. A schematization that highlights the main zones is superimposed to the CFD image.

The convective delay time τ_c, namely the time prior to the first detection of the tracer, is slightly higher in the oxyfuel case (for exact values compare Table 3). This is caused primarily by the higher flow rates for the air case and its different mixing between the seeded primary flow and secondary/tertiary flows. Differences in the mixing are similarly evident from the time the system needs until half of the final concentration value is detected, $\tau_{0.5*C\infty}$. This quantity is slightly higher for the air case despite its lower τ_c, underlying the sharper increase in tracer concentration observable in Figure 3 for the oxyfuel case compared to the smoother increase when operating with air.

Another difference between the two operation conditions lies in the different way they approach the final concentration. For NRAir the tracer concentration rises smoothly until the final concentration is reached. In contrast, the oxyfuel operation point exhibits a steep increase initially, then approaches the final value in a stepwise manner, slower compared to the other case.

Table 3 – Characteristic times

τ_i [s]	NRAIR	NR30
τ_c	0.51	0.6
$\tau_{0.5*C\infty}$	1.47	1.23

The sharp initial increase followed by the retarded rise suggests a more pronounced influence of phenomena occurring in parallel that are characterized by different time scales. Referring to Figure 4, different characteristic time scales might be distinguished in the segregated zone and the diluted zone (DZ). In particular, this might be due to a smaller amount of tracer mixing in that zone, which is in turn subjected to longer residence times. In contrast, these phenomena might be as well present while using air, but their characteristic times might not be so different. In addition, the shape of the response in the latter case suggests a larger size of the overall stirred region inside the combustor, leading to a less steep increase [17].

Building on these considerations and the main flow structures in Figure 4, the design of a CRN followed a stepwise approach: based on the simple modelling in [9], a first, simple network was tested. Complexities were gradually added, to take into account more features of the flow field. The selected network, shown in Figure 5, is the one that could fit both air and oxyfuel operation points, exhibiting only one global minimum.

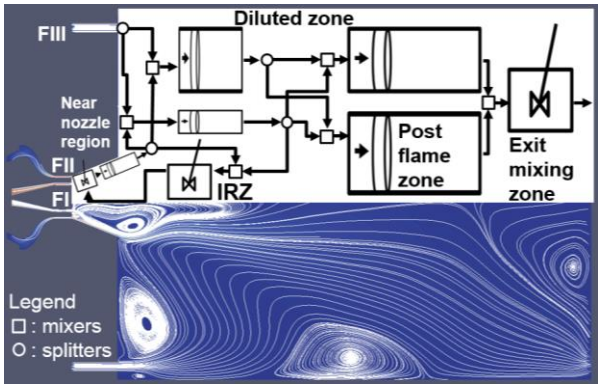

Figure 5 – CNR superimposed to the mean flow field.

It aims to describe the flow and mixing characteristics in a simple way, still addressing the main features. In particular, it takes into account:

- a part of the inlet flow bypassing the internal recirculation zone, represented by a series of a CSTR for the mixing in the near nozzle region [11, 10], and two PFR to describe the jet-like features of this flow;
- an internal recirculation zone (IRZ), receiving flow from the two PFR of the bypass region;
- a segregated post flame zone (PFZ), exemplified by a single PFR;
- a final recirculation zone at the exit;
- PFRs parallel to the central zone to represent the DZ, with flow exchange with the central flow zone. This parallel arrangement allows modelling of different characteristic times in the PFZ and the DZ. The possibility that the tracer does not fill all of the volume in the DZ for mixing (i.e., presence of dead volumes) is also considered.

Experimental and modelling results of $F(t)$ are compared in Figure 6, showing a reasonable agreement. The parallel arrangement in the reactor network representing the flow in the central zone and in the DZ suits both operational conditions.

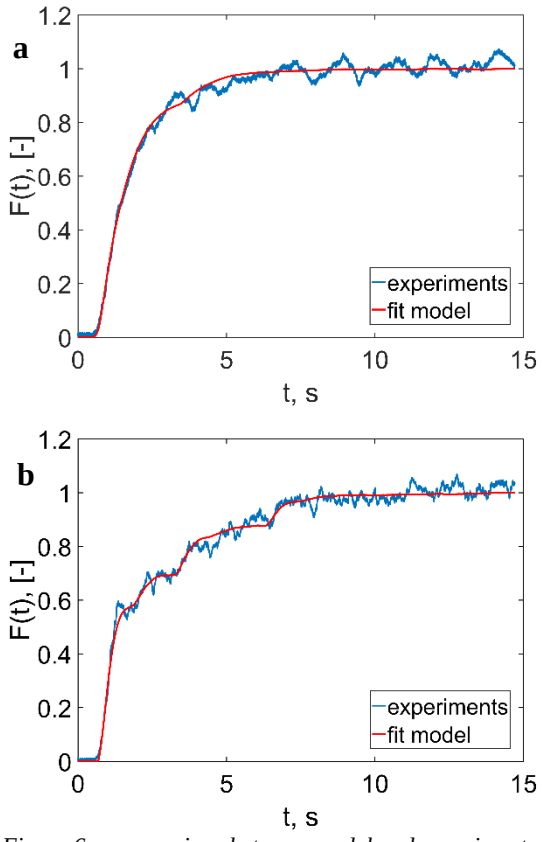

Figure 6 – comparison between model and experiment
***a** – NRAir*
***b** – NR30*

In a next step, RTDs calculated from the model are compared in Figure 7. As expected from the results in Figure 7, the air case shows a more unimodal shape, while the oxyfuel case exhibits distinct peaks.

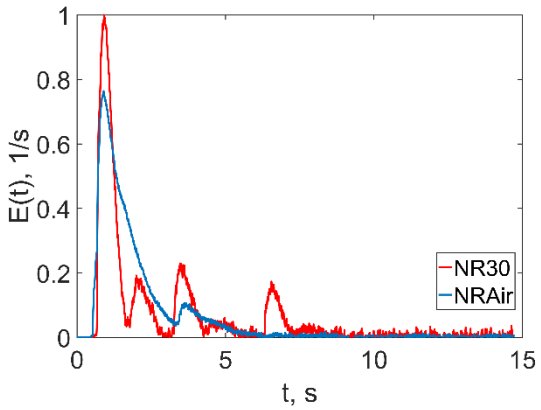

Figure 7 – calculated residence time distribution

The presence of multiple peaks is typical of PFRs in parallel, and can be related to the dispersion of the tracer in zones with different characteristic times. In particular, several parameters can be calculated from the RTD, listed in Table 4.

Table 4 – Characteristic properties extracted from modelled RTDs.

	NRAir	**NR30**	**NRAir** [22]	**NR30** [22]
τ_m, [s]	1.9	2.5	1.9	2.5
σ_θ^2, [s^2]	0.54	0.80		
D/uL, [-]	0.45	1.37	0.303	1.11
τ_d, [s]	1.4	1.9		

τ_m and σ_θ^2 are, respectively, the mean residence time of the combustor and its variance, [17]. The variance is related to the axial dispersion coefficient D, which represents the spreading process.

The spreading process can be further quantified by:

$$D/uL \qquad (6)$$

where D is the dispersion coefficient, u the average speed in the stream wise direction and L the length of the vessel. The value of this dimensionless group is calculated according to equation (7), using the value of the second order moment of the RTD, σ_θ^2 [17].

$$\sigma_\theta^2 = 2\left(\frac{D}{uL}\right) - 2\left(\frac{D}{uL}\right)^2\left[1 - e^{-\frac{uL}{D}}\right] \qquad (7)$$

As reported in Table 4, its value for the oxyfuel case is higher, confirming a higher dispersion compared to the air case.

This behaviour is related to the different molecular weights of air (29 g/mol) and oxyfuel (40 g/mol). According to [23],

$$D = \text{[illegible]} + C/\text{[illegible]} \qquad (8)$$

In equation (8), $\mathcal{D}$ is the mass diffusivity and C is a constant that depends on the flow.

The diffusion coefficient $\mathcal{D}$ is inversely proportional to the molecular weight, and it is thus smaller for an oxyfuel environment. Therefore, the mass transfer in the oxyfuel case is more influenced by convection causing a larger spreading rate.

The influence of the dispersion on the mean residence time of the process is expressed by [13]:

$$\tau_m = \tau_c + \tau_d \qquad (9)$$

where τ_d denotes the dispersive time delay. τ_d, obtained as the difference between τ_m and τ_c, is also listed in Table 4, confirming that a higher dispersion characterizes oxyfuel environments, also reported in [22].

Conclusions

A simple chemical reactors network model for a close to reality configuration has been developed building on the interpretation of measured residence time distributions in terms of main flow structures. Air and oxyfuel atmospheres have been investigated. The model is able to reasonably represent the mixing characteristics for both cases. In this way, differences in the mixing characteristics of air and oxyfuel operation were identified. In particular, higher dispersion is present for oxyfuel operation, while the importance of zones in which perfect mixing can be assumed is greater for the air case.

Acknowledgments

The authors thank the Deutsche Forschungsgemeinschaft for its support through CRC/Transregio 129. M. A. Agizza and G. Bagheri are grateful for financial support through European Union's Horizon 2020 research and innovation program under the Marie Sklodowska-Curie grant agreement No 643134. A. Dreizler is grateful for support by the Gottfried Wilhelm Leibniz Program of the Deutsche Forschungsgemeinschaft.

References

[1] World Energy Council , "World Energy Resources, Survey 2013," 'Used by permission of the World Energy Council' , 2013.

[2] Internal Energy Agency, "Energy and Air Pollution 2016, World Energy Outlook Special Report," 2016.

[3] L. Chen, S. Z. Yong, and A. F.Ghoniem, *Prog. Energy Combust. Sci.* 38(2), (2012), 156-214.

[4] A. B. Lebedev, A. N. Secundov, A. M. Starik, N. S. Titova, and A. M. Schepin, *Proc. Comb. Inst.* 32, (2009), 2941-2947.

[5] G. Sturgess and D. T. Shouse, *AIAA paper*, (1996), 96-3125.

[6] T. Faravelli, L. Bua, A. Frassoldati, A. Antifora, L. Tognotti and E. Ranzi, *Comp. Chem. Eng.* 25(4), (2001), 613-618.

[7] N. Rizk and H. C. Mongia, *ASME 1992 International Gas Turbine and Aeroengine Congress and Exposition*, V003T06A023-V003T06A023.

[8] A. Andreini and B. Facchini, *ASME Turbo Expo 2002: Power for Land, Sea, and Air*, 271-281.

[9] J. M. Beer and K. B. Lee, *Symp. (Int.) on Comb.* 10, 1965,1187-1202.

[10] R. P. Van Der Lans, P. Glarborg, K. Dam-Johansen and P. S. Larsen, *Chem. Eng. Sci.* vol. 52, 1997, 2743-2756.

[11] L. S. Pedersen, P. Breithauptb, K. D. Johansen and R. Weber, *Comb. Sci. Tech.* 127, 1997, 251-273.

[12] I. V. Novosselov, *Phd Diss.*, 2006.

[13] K. Göckeler, S. Terhaar, A. Lacarelle and C. O. Paschereit, *Proc. 41st AIAA Fluid Dynamics Conference and Exhibit*, 2011.

[14] K. Göckeler, S. Terhaar and C. O. Paschereit, *J. ENG. GAS TURB. POWER*, 136, 2014.

[15] M. De Joannon, P. Sabia, G. Sorrentino, P. Bozza and R. Ragucci, *Proc. Comb. Inst.*, 2016.

[16] A. De Toni, T. Hayashi and P. Schneider, *J Brazil. Soc. Mech. Sci. Eng.* 35, 2013, 199-206.

[17] O. Levenspiel, Chemical Rection Engineering, John Wiley & Sons, third edition, 1999.

[18] D. G. Nicol, R. C. Steele, N. M. Marinov and P. C. Malte, *J. ENG. GAS TURB. POWER* 117, 1995, 100-111.

[19] P. V. Danckwerts, *Chem. Eng. Sci.* 2, 1953, 1-13.

[20] L. G. Becker, H. Kosaka, B. Böhm, S. Doost, R. Knappstein, M. Habermehl, R. Kneer, J. Janicka and A. Dreizler, *Fuel*, 2016.

[21] A. S. Doost, F. Ries, L. G. Becker, S. Bürkle, S. Wagner, V. Ebert, A. Dreizler, F. di Mare, A. Sadiki and J. Janicka, *Chem. Eng. Sci.* 156, 2016, 97-114.

[22] S. Bürkle, L. G. Becker, M. A. Agizza, A. Dreizler, V. Ebert and S. Wagner, *Submitted to Experiments in Fluids*, 2017.

[23] W. M. Deen, Analysis of Transport Phenomena, Topics in Chemical Engineering, vol. 3, 1998, Oxford University Press, New York.